AMERICAN JOURNAL OF PHYSIOLOGY
HEART AND CIRCULATORY PHYSIOLOGY

Am J Physiol Heart Circ Physiol 327: H847–H858, 2024.
First published August 9, 2024; doi:10.1152/ajpheart.00341.2024

RESEARCH ARTICLE

Vascular Contributions to Human Disease

Sex differences in gray matter, white matter, and regional brain perfusion in young, healthy adults

Jessica D. Muer,[1] Kaylin D. Didier,[1] Brett M. Wannebo,[1] Sophie Sanchez,[1] Hedyeh Khademi Motlagh,[1] Travis L. Haley,[1] Katrina J. Carter,[1] Nile F. Banks,[1] Marlowe W. Eldridge,[2] Ronald C. Serlin,[5] Oliver Wieben,[3,4] and William G. Schrage[1]

[1]*Department of Kinesiology, University of Wisconsin-Madison, Madison, Wisconsin, United States;* [2]*Department of Pediatrics, University of Wisconsin-Madison, Madison, Wisconsin, United States;* [3]*Department of Radiology, University of Wisconsin-Madison, Madison, Wisconsin, United States;* [4]*Department of Medical Physics, University of Wisconsin-Madison, Madison, Wisconsin, United States; and* [5]*Department of Educational Physcology, University of Wisconsin-Madison, Madison, Wisconsin, United States*

Abstract

Cerebrovascular and neurological diseases exhibit sex-specific patterns in prevalence, severity, and regional specificity, some of which are associated with altered cerebral blood flow (CBF). Females often exhibit higher resting CBF, but understanding the impact of sex per se on CBF is hampered by study variability in age, comorbidities, medications, and control for menstrual cycle or hormone therapies. A majority of studies report whole brain CBF without differentiating between gray and white matter or without assessing regional CBF. Thus fundamental sex differences in regional or whole brain CBF remain unclarified. While controlling for the above confounders, we tested the hypothesis that females will exhibit higher total gray and white matter perfusion as well as regional gray matter perfusion. Adults 18–30 yr old (females = 22 and males = 26) were studied using arterial spin labeling (ASL) magnetic resonance imaging (MRI) scans followed by computational anatomy toolbox (CAT12) analysis in statistical parametric mapping (SPM12) to quantify CBF relative to brain volume. Females displayed 40% higher perfusion globally (females = 62 ± 9 and males = 45 ± 10 mL/100 g/min, $P < 0.001$), gray matter (females = 75 ± 11 and males = 54 ± 12 mL/100 g/min, $P < 0.001$), and white matter (females = 44 ± 6 and males = 32 ± 7 mL/100 g/min, $P < 0.001$). Females exhibited greater perfusion than males in 67 of the 68 regions tested, ranging from 14% to 66% higher. A second MRI approach (4-dimensional flow) focused on large arteries confirmed the sex difference in global CBF. These data indicate strikingly higher basal CBF in females at global, gray, and white matter levels and across dozens of brain regions and offer new clarity into fundamental sex differences in global and regional CBF regulation before aging or pathology.

NEW & NOTEWORTHY MRI used to measure cerebral blood flow (CBF) in gray matter, white matter, and 68 regions in healthy men and women. This study demonstrated that CBF is 40% higher in women, the highest sex difference reported, when controlling for numerous important clinical confounders like age, smoking, menstrual cycle, comorbidities, and medications.

brain lobes; brain perfusion; gray matter perfusion; regional differences; sex differences

INTRODUCTION

Millions of people in the United States are impacted by cerebrovascular, neurological, and neurodegenerative diseases, many of which are associated with altered cerebral blood flow (CBF) (1–4). Several brain pathologies also exhibit sex differences in prevalence, prognosis, and severity. For example, in females, lower CBF is associated with depression severity (5), and altered CBF is associated with migraines (6). In contrast, hypertension (7, 8), sleep apnea (9, 10), and schizophrenia (11–13) are associated with alterations in CBF that are more prevalent in males. Collectively, these observations suggest that sex-specific CBF patterns may help to understand or treat brain pathologies.

A growing number of studies in healthy adults indicate that females display higher CBF than males (12, 14–21). However, a clear understanding of the true magnitude of sex differences in CBF remains difficult to establish because of numerous factors known to influence CBF, including aging, comorbidities, lack of control of menstrual cycle in females, and inclusion of subjects taking medications, including hormone contraceptives. First, CBF declines with age in both

Correspondence: K. D. Didier (didier2@wisc.edu).
Submitted 23 May 2024 / Revised 26 July 2024 / Accepted 5 August 2024

sexes (14, 21), making it difficult to separate age from age-sex interactions. Second, subject characteristics in some prior studies (8, 22–27) suggest obesity and/or hypertension existed, and these and other comorbidities are linked to altered CBF. Third, evidence suggests that CBF varies across the menstrual cycle (20, 28, 29), and most studies do not strictly control for this (14, 30). Similarly, hormonal contraception in females may influence CBF, as several vascular beds, including skin (31–33) and skeletal muscle (34), are known to be influenced by oral contraceptive pills. Varying levels of cardiorespiratory fitness can influence CBF (35, 36). All of these factors could under- or overrepresent essential sex differences in cerebral perfusion. To our knowledge, no study has tested for sex differences in CBF while attempting to limit the impact of these important confounding factors, leaving a gap in our understanding of the true magnitude of sex differences in CBF.

Another consideration is that only a few studies have separated gray matter (GM) from white matter (WM) CBF. This is noteworthy as gray matter perfusion is much higher than white matter (37), and females may exhibit a different percentage of gray and white matter volume (38–40), which could mask true sex differences in CBF. Furthermore, findings are limited because of some of the design limitations noted above (age, obesity, and cardiovascular risk factors). Finally, some studies only assess blood velocity (not CBF) in a single middle cerebral artery (MCA) (15, 41–45), which does not allow for whole brain CBF measures or exploration of regional differences.

Identifying sex differences in regional CBF may be insightful for preventative and diagnostic tools because several cerebral regions exhibit structural and/or perfusion changes in pathological states, but there is limited information regarding this. For example, Alzheimer's disease is associated with decreased CBF in the hippocampus, amygdala, and parahippocampus (46–48). In addition, depression (49) and anxiety (50, 51) are associated with localized changes in CBF. Therefore, the goal of this study was to assess CBF in multiple small regions of the brain to identify sex differences that may not be apparent in global perfusion values while controlling for numerous conditions that may alter regional CBF. The purpose of this study was to examine potential sex differences in gray matter, white matter, and regional perfusion in young, healthy adults while controlling for several key factors known to influence CBF. We tested the hypotheses that females will exhibit higher CBF in *1*) the whole brain, *2*) gray matter, *3*) white matter, and *4*) the majority of smaller gray matter regions.

METHODS

Subjects

Fifty-one young, healthy adults (22 females) voluntarily participated in this study. Written informed consent was obtained before participation in the study. All procedures were approved by the University of Wisconsin-Madison Health Sciences Institutional Review Board and were in accordance with the Declaration of Helsinki [registered in the ClinicalTrials.gov database (ID: NCT04265053)].

All subjects completed an initial screening visit to determine eligibility. Subjects completed a medical history questionnaire, MRI safety questionnaire, venipuncture, pregnancy test (females only), and anthropometric measurements (height, weight, waist, and hip circumference). Brachial artery blood pressure was measured using an automated sphygmomanometer (Datex Ohmeda), and the lowest of three measurements was used to assess eligibility.

All subjects were 18–30 yr old with a systolic blood pressure (SBP) of $\leq$125 mmHg, diastolic blood pressure (DBP) of $\leq$80 mmHg, body mass index (BMI) of $\leq$25 kg/m^2, blood glucose of $<$100 mg/dL, low-density lipoprotein (LDL) of $<$130 mg/dL, and triglycerides of $<$150 mg/dL. Exclusion criteria included smoking; taking any cardiovascular, hormonal, or metabolic medication; any overt cardiovascular, neurological, depression/anxiety, autoimmune, or reproductive disorders; and MRI contraindications. Females were not pregnant or lactating, were regularly menstruating, were free of any reproductive disorders, and were not currently taking hormonal contraceptives for at least 6 mo.

MRI Study Visit

Previsit procedures.

Subjects attended a single MRI visit after fasting for $\geq$8 h, as well as abstaining from vigorous exercise, alcohol, caffeine, and nonsteroidal anti-inflammatory drugs for $\geq$24 h. Female subjects were tested in the early follicular phase (*days 1–7*) of their menstrual cycle. Negative pregnancy status was confirmed again on the day of the study.

Instrumentation. MRI scanning occurred in a three-Tesla (3-T) MRI system with a 48-channel head coil (Discovery MR750; GE Healthcare, Waukesha, WI). Subjects were instrumented with a respiratory gating belt, pulse oximeter, and blood pressure cuff (automated sphygmomanometer). Breath-by-breath end-tidal carbon dioxide (ET_{CO_2}) was assessed via capnography.

Protocol. Subjects were instructed to lay still and awake with their eyes closed during the MRI scans. A T1-weighted image set, pseudocontinuous arterial spin labeling (pcASL), and four-dimensional (4-D) phase contrast vastly undersampled isotropic projection reconstruction (PC-VIPR) flow MRI scans were completed (~10 min) while the subject breathed room air.

The study team visually monitored the subject's vital signs during the study visit (Medrad Veris MR Vital Signs Patient Monitor; Bayer Healthcare, Whippany, NJ) and recorded heart rate (HR) and ET_{CO_2} every minute during the T1, pcASL, and PC-VIPR scans. Mean arterial blood pressure (MAP), oxygen saturation (Sp_{O_2}), and respiratory rate were recorded during the last minute of each scan. HR and ET_{CO_2} values within each scan were averaged.

T1 scan parameters.

A T1-weighted MRI scan was completed using an ADNI 3 protocol on a 3-T GE 750 scanner. An accelerated sagittal three-dimensional (3-D) IR-FSPGR (inversion recovery fast spoiled gradient echo) sequence was completed and then used for brain structure analysis. Parameters of the scan were flip angle = 11, repetition time = 7.2 ms, echo time = 2.9 ms, inversion time = 400 ms, field of view = 27 cm, slice thickness = 1 mm, matrix size = 256 × 256, and number of excitations = 1. All T1 images were reviewed independently by two study team members to remove any subjects who demonstrated motion artifacts that could

reduce the validity of CBF measures, resulting in the removal of two subjects.

Pseudocontinuous arterial spin labeling parameters. A background (pcASL) was used to assess cerebral perfusion and perform image registration. The pcASL sequence featured a 3-D fast spin-echo spiral readout using a stack of variable-density 5-ms readout and eight interleaves. Parameters of the scan were flip angle = 111, repetition time = 6,031 ms, echo time = 64.8 ms, inversion time = 1,000 ms, field of view = 240 mm, slice thickness = 4-mm no gap, matrix size = 128 × 128, number of excitations = 1, and labeling radiofrequency amplitude = 0.24 mG. The postlabeling delay was 2,025 ms. During the same imaging sequence/image slab location as the pcASL, we acquired a fluid-suppressed proton density (PD) scan but without radiofrequency labeling preparation.

Four-dimensional flow magnetic resonance imaging. In addition to ASL MRI, we used a second method to verify differences in global CBF using 4-D flow MRI. 4-D flow MRI was obtained with PC-VIPR to quantify blood flow concurrently in 11 separate cerebral conduit arteries. For this project, we focused on CBF through the left and right internal carotid arteries combined with the basilar artery. PC-VIPR (52, 53) is a validated MRI sequence (54, 55) that simultaneously assesses cerebrovascular flow and vessel lumens in multiple vessels and is used in various applications, including Alzheimer's disease (56), insulin resistance (57), and hypoxia challenges (42). The following scan parameters were used imaging volume = $22 \times 22 \times 22$ cm^3, acquired isotropic spatial resolution = (0.69 mm^3), scan time = 5 min 38 s, velocity encoding (V_{enc}) = 100 cm/s, flip angle = 8°, and repetition time/echo time = 6.7/2.8 ms (20 reconstructed cardiac time frames using retrospective cardiac gating and temporal view sharing) (58). All PC-VIPR images were reviewed independently to remove any subjects who demonstrated motion artifacts that could reduce the validity of CBF measures, resulting in the removal of three subjects (2 females).

Data Processing

pcASL analysis. Cerebral T1-weighted and pcASL perfusion images were analyzed in MATLAB (The Mathworks, Natick, MA) using the Computational Anatomy Toolbox (CAT12) for Statistical Parametric Mapping version 12 (SPM12). CAT12 data were provided for use in the MICCAI 2012 Grand Challenge and Workshop on Multi-Atlas Labeling (B. Landman and S. Warfield, MICCAI 2012 workshop on multiatlas labeling, in MICCAI Grand Challenge and Workshop on Multi-Atlas Labeling, CreateSpace Independent Publishing Platform, Nice, France, 2012). The data were released under the creative commons attribution-noncommercial license (CCBY-NC) with no end date. Original MRI scans were from OASIS (https://www.oasis-brains.org/). Labelings were provided by Neuromorphometrics, Inc. (http://Neuromorphometrics.com/) under academic subscription (59).

First, pcASL images were transit time corrected. T1-weighted digital imaging and communications in medicine (DICOM) and pcASL DICOM images were converted into Neuroimaging Informatics Technology Initiative (NIfTI) files and then uploaded into MATLAB. CAT12 was used to optimally resample T1-weighted scans and correct for noise, bias, and global intensities. T1-weighted scans were then segmented to obtain partial gray matter and white matter masks in native space (threshold = 0.8). T1-weighted scans were also regionally segmented relative to the neuromorphometrics atlas in MNI152NLin2009cAsym space (MNI; Montreal Neurological Institute) (59). The partial gray matter masks were coregistered to the ASL scans using an affine transformation and smoothed using a 7-mm full width at half-maximum Gaussian kernel. Total gray matter and total white matter perfusion were assessed in native space relative to the coregistered images. Regional perfusion was assessed relative to the neuromorphometrics atlas (59). Scan quality was assessed by CAT12 quality control parameters, and two authors independently completed a visual analysis of T1 and ASL scans. ASL data were excluded if either author identified any of the following conditions: motion artifact, improper fitting of the brain to normalized MNI space, or inhomogeneity artifact. Two subjects were removed because of poor scan quality.

Flow (PC-VIPR) analysis. PC-VIPR data were processed using custom in-house centerline processing software developed in MATLAB (Mathworks, Natick, MA), which provides a reliable measurement of cerebral artery blood flow (54). Centerline processing software segments individual vessels in a plane perpendicular to the vessel path, one voxel in width (0.69 mm). At each voxel plane, multiple measurements, including time-averaged velocity, cross-sectional area (CSA), and flow measures for the vessel, are collected. For each vessel segment, three to five consecutive cross sections were analyzed and averaged for measures of flow, velocity, and CSA. Three cerebral conduit arteries were assessed for 20 female and 25 male subjects to provide total CBF: the left and right internal carotid arteries and the basilar artery. The following standardized locations were used to ensure laminar flow and obtain reliable measurements: internal carotid arteries were measured in the middle straight portion of the C4 segment (60), and the basilar artery was measured 4–7 mm (~5–10 voxels) from the junction with the vertebral artery. Total CBF was calculated as the sum of the left and right internal carotid arteries and the basilar artery. 4-D PC-VPIR scan quality was assessed by two authors independently. Scans were reviewed to determine if the data contained poor T1-weighted image quality, poor vessel visualization (as indicated by an absence of voxels), or significant flow inversion indicated by three of five consecutive voxels. No subjects were removed.

Cerebrovascular conductance and cerebral delivery of oxygen calculations. Cerebrovascular conductance was calculated as CVC = (CBF/MAP) × 100. Cerebral delivery of oxygen was calculated as CDO_2 = blood flow (BF) × Ca_{O_2}, whereas BF (mL/min) = neuronal density × matter volume × CBF. A neuronal density of 1.05 g/cm^3 (gray matter) and 1.04 g/cm^3 (white matter) was assumed based on reported averages (61). Ca_{O_2} = (1.34 mL O_2/gHb × [Hb] × Sp_{O_2}) + (Pa_{O_2} × 0.003 mL O_2/mL blood/mmHg), where Hb is hemoglobin and an arterial partial pressure of oxygen (Pa_{O_2}) of 100 mmHg arterial O_2 pressure was assumed.

Table 1. *Subject characteristics*

	Female	Male	*P* Value
n	22	26	
Age, yr	22 ± 3	23 ± 4	0.28
Height, cm	166 ± 6	177 ± 8*	<0.01
Weight, kg	60 ± 6	71 ± 6*	<0.01
BMI, kg/cm^2	21.8 ± 1.6	22.5 ± 1.5	0.06
SBP, mmHg	107 ± 7	114 ± 8*	<0.01
DBP, mmHg	66 ± 7	68 ± 5	0.11
MAP, mmHg	80 ± 7	83 ± 5*	0.02
Glucose, mg/dL	76 ± 8	81 ± 14	0.06
Cholesterol, mg/dL			
Total	150 ± 30	138 ± 32	0.09
HDL	67 ± 18	55 ± 12*	<0.01
LDL	72 ± 24	70 ± 25	0.4
Triglycerides, mg/dL	59 ± 10	68 ± 20*	0.02
Hemoglobin, g/dL	12 ± 2	15 ± 2*	<0.01

Values are means ± SD. BMI, body mass index; SBP, systolic blood pressure; DBP, diastolic blood pressure; MAP, mean arterial blood pressure; HDL, high-density lipoprotein; LDL, low-density lipoprotein. Hemoglobin, $n = 15$ females and 17 males. *$P < 0.05$, significant difference between female and male participants, using unpaired *t* tests.

Statistical Analysis

Data were assessed with Shapiro-Wilk normality tests and Brown–Forsythe variance tests, then unpaired, one-tailed Student's *t* tests were used to evaluate differences between sexes using Sigma-Plot 13.0 (Systat Software, Point Richmond, CA). All regional data are averages of left and right perfusion values. Significance was set at $P < 0.05$.

Significant differences between groups (male vs. female) were assessed using an unpaired *t* test, and Shaffer's method (62, 63) was used to control the error rate for multiple comparisons. The study has a two-group (sex) design across 68 brain regions. Its multivariate nature was accommodated by forming summary measures. For example, six CBF totals (CBF_{total}) were calculated for six lobes/larger regions (brainstem/cerebellum, subcortical, frontal, temporal, parietal, and occipital), each comprising the sum of 6–19 brain regions per lobe (e.g., hippocampus within the temporal lobe). All the regions within a lobe are anatomically related and likely rely on similar blood supply. The analysis was based on differences between sexes of the summary measures as dependent variables, and the analysis proceeded in a sequential fashion as described by Shaffer's method, with the most significant of the constituent tests being assigned $\alpha = 0.05/6 = 0.0083$. Of the remaining five brain regions in that lobe, assigned $\alpha = 0.05/5 = 0.01$, then $0.05/4 = 0.0125$, and so on until finally 0.05/1. In the present study, all the composite tests were significant, and therefore, we conducted the Shaffer sequential method within each lobe. An example is the parietal lobe, which has eight regions. Since the composite test was significant, the most significant of the constituent tests was assigned $\alpha/(n\text{-}1) = 0.05/7 = 0.0071$. Of the remaining seven brain regions in that lobe, assigned $\alpha/(n\text{-}1) = 0.05/7 = 0.0071$, then $\alpha/(n\text{-}2) = 0.05/6 = 0.0083$, and so on until finally $\alpha/(n\text{-}7) = 0.05/1$. If any of the subsequent tests are nonsignificant, the sequence will be halted.

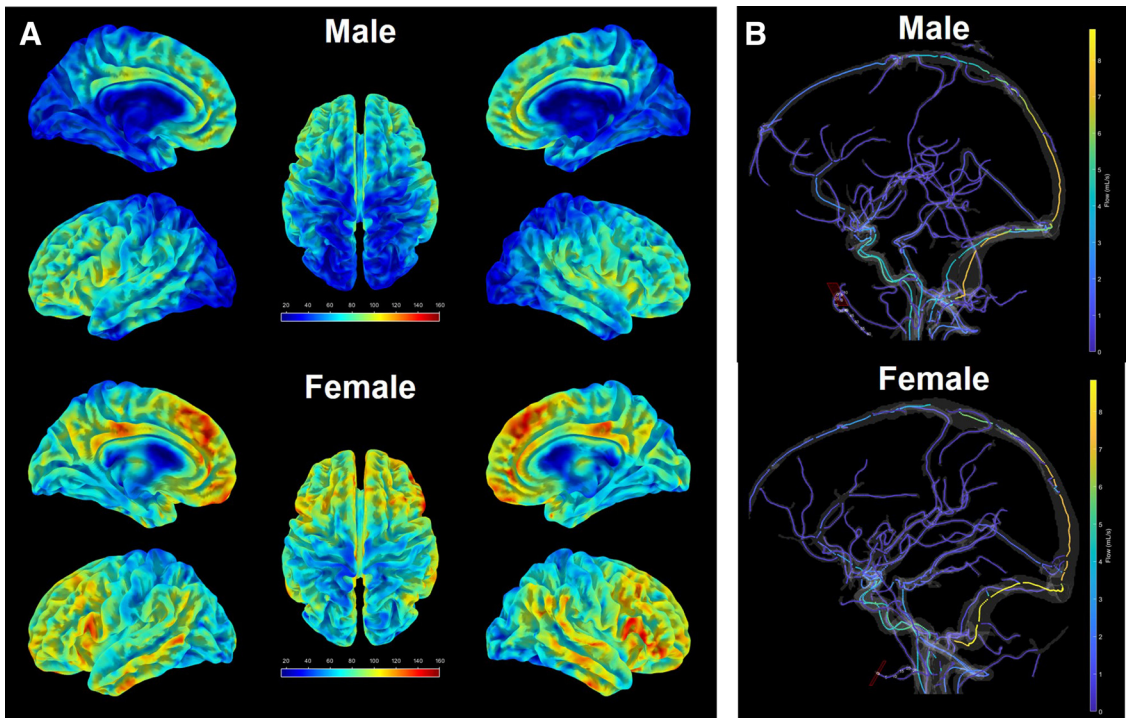

Figure 1. Whole brain magnetic resonance imaging (MRI) perfusion images for 1 male and 1 female subject that are representative of the group mean. *A*: coregistered pseudocontinuous arterial spin labeling (pcASL) and T1 scans normalized to the Montreal Neurological Institute (MNI) space. Yellow-to-red coloring represents more blood flow (mL/min/100 g) to the region, and green-to-blue coloring represents less blood flow to that region. *B*: representative image from 4-dimensional (4-D) flow analysis [phase contrast vastly undersampled isotropic projection reconstruction (PC-VIPR); see METHODS]. Yellow-to-green coloring represents more blood flow (mL/s) to the vessel, and purple-to-blue coloring represents less blood flow to that vessel. Images are lateral perspectives.

Table 2. *Whole brain characteristics*

	Female	Male	*P* Value
n	22	26	
Volume, cm^3			
Total	1,193 ± 103	1,326 ± 79*	<0.001
GM	708 ± 58	786 ± 51*	<0.001
WM	486 ± 51	541 ± 41*	<0.001
GM/WM ratio	1.5 ± 0.1	1.46 ± 0.1	0.44
Perfusion, mL/100 g/min			
GM	75 ± 11	54 ± 12*	<0.001
WM	44 ± 6	32 ± 7*	<0.001
ASL total	62 ± 9	45 ± 10*	<0.001
4-D flow	56 ± 9	45 ± 7*	<0.001

Values are means ± SD. GM, gray matter; WM, white matter; ASL, arterial spin labeling; 4-D, 4-dimensional. *$P < 0.05$, significant difference between female and male participants, using unpaired *t* tests.

Student's *t* tests were used to assess sex differences in subject characteristics and hemodynamic parameters. All data are expressed as means ± SD.

RESULTS

Subject Characteristics

Subject characteristics are summarized in Table 1. By design, all subjects had a healthy BMI, normotensive blood pressure, as well as glucose and lipid levels associated with low cardiovascular or cerebrovascular disease risk. Males exhibited higher SBP ($P < 0.01$) and MAP ($P = 0.02$), but both sexes were normotensive (<125/85 mmHg). Finally, females had significantly higher levels of HDL cholesterol ($P < 0.01$), whereas males had higher triglyceride ($P = 0.02$) and hemoglobin concentrations ($P < 0.01$).

Whole Brain Volume and Perfusion

Examples of pcASL and 4-D flow analyses are displayed in Fig. 1. The MRI scans for one male and one female were selected because their results most similarly represent the mean value for each method and provide the best representation of mean sex differences. Males exhibited larger global ($P < 0.001$), gray matter ($P < 0.001$), and white matter volumes ($P < 0.001$) (Table 2). However, there was no significant sex difference in the ratio of gray matter volume to white matter volume ($P = 0.44$) (Table 2). Data from pcASL scans indicated that females exhibited ~40% higher global brain perfusion, global gray matter perfusion, and global white matter perfusion than males (Table 2; Fig. 2). Volumetric flow (4-D flow) data indicated CBF was 56 ± 9 mL/min in females and 45 ± 7 mL/min in males ($P < 0.001$), and when normalized to individual total brain volume, females still displayed 21% higher relative flow (Table 2; Fig. 2).

Regional Perfusion

Regional perfusion values for 68 regions are presented in Table 3 with a subsample presented in Fig. 3. On average, females exhibited 40% higher perfusion in brain regions tested (range: 14%–66%; Fig. 4). Sixty-seven of the 68 regions displayed higher perfusion in females (Table 3).

Respiratory and Hemodynamic Values

Hemodynamic values are presented in Supplemental Table S1 (all Supplemental material is available at https://doi.org/10.6084/m9.figshare.26383753). Average heart rate during the pcASL scan was not different between sexes ($P = 0.05$). However, average $ETCO_2$ ($P < 0.001$) and mean arterial pressure ($P = 0.01$) were significantly higher in males during the pcASL scan. Since MAP was different between sexes, we also calculated cerebrovascular conductance (CVC, where CVC = CBF/MAP) (Supplemental Table S2). All global values and regions showed significantly higher CVC in females ($P < 0.001$). Total cerebral delivery of oxygen (CDO_2) was not significantly different between sexes, as cerebral arterial oxygen content (Ca_{O_2}) was higher in males, but CBF (measured via 4-D flow) was greater in females (Supplemental Table S3).

DISCUSSION

Current findings support the hypothesis that healthy younger females exhibit substantially higher resting perfusion in gray matter, white matter, and all small regions of the brain compared with males. This sex difference is notable due to the rigorous control of confounding factors that might influence CBF either directly or indirectly via a sex- or comorbid-specific vascular mechanism. The present data plainly identify large fundamental sex differences in CBF across the entire brain, which could be useful in understanding the pathophysiology of various brain conditions known to exhibit sex-specific and region-specific pathophysiology.

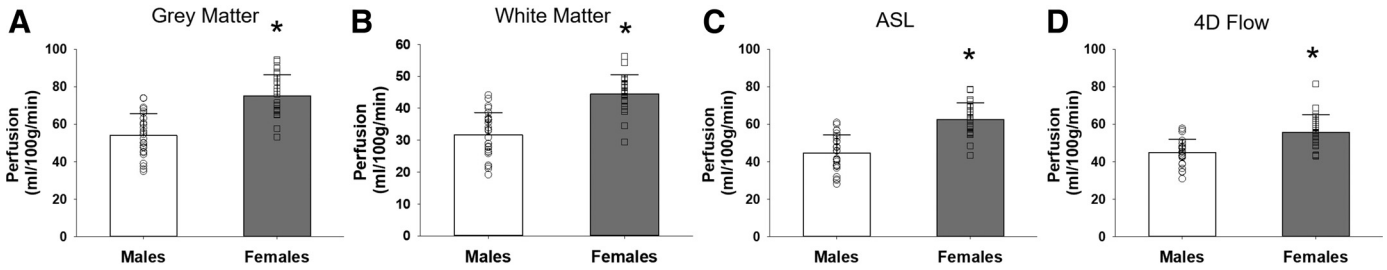

Figure 2. Whole brain perfusion. *A*: gray matter perfusion. *B*: white matter perfusion. *C*: total arterial spin labeling (ASL) perfusion. *D*: total perfusion by 4-dimensional (4-D) flow. Open circles represent individual data points for males ($n = 26$) and females ($n = 22$). *$P < 0.05$, significant difference between males and females, using unpaired *t* tests.

Table 3. *Regional perfusion of regions*

Region	Female	Male	*P* Value
n	22	26	
Brain stem/cerebellum			
Brain stem	42 ± 6	31 ± 7	<0.0001
Cerebellum exterior	66 ± 10	44 ± 10	<0.0001
Cerebellum white matter	44 ± 6	30 ± 7	<0.0001
Cerebellar vermal lobules I–V	46 ± 11	29 ± 10	<0.0001
Cerebellar vermal lobules VI–VII	53 ± 11	32 ± 11	<0.0001
Cerebellar vermal lobules VIII–X	59 ± 11	40 ± 10	<0.0001
Subcortical regions			
Amygdala	54 ± 8	44 ± 9	<0.0001
Thalamus	56 ± 9	39 ± 9	<0.0001
Ventral diencephalon	45 ± 7	34 ± 7	<0.0001
Optic chiasm	43 ± 9	38 ± 9	0.026
Anterior cingulate gyrus	90 ± 12	71 ± 13	<0.0001
Middle cingulate gyrus	85 ± 13	64 ± 12	<0.0001
Posterior cingulate gyrus	80 ± 14	55 ± 13	<0.0001
Subcallosal area	68 ± 10	56 ± 10	0.0001
Accumbens	70 ± 10	59 ± 10	0.0001
Caudate	57 ± 8	47 ± 7	<0.0001
Pallidum	42 ± 6	36 ± 6	0.0003
Putamen	62 ± 9	52 ± 8	<0.0001
Frontal lobe			
Basal forebrain	63 ± 8	53 ± 10	0.0001
Anterior orbital gyrus	86 ± 13	66 ± 14	<0.0001
Central operculum	80 ± 11	65 ± 12	<0.0001
Frontal operculum	90 ± 13	72 ± 14	<0.0001
Frontal pole	91 ± 16	72 ± 15	<0.0001
Gyrus rectus	89 ± 12	72 ± 13	<0.0001
Lateral orbital gyrus	87 ± 13	69 ± 14	<0.0001
Medial frontal cortex	94 ± 13	75 ± 12	<0.0001
Middle frontal gyrus	86 ± 16	63 ± 15	<0.0001
Medial orbital gyrus	80 ± 10	66 ± 11	<0.0001
Precentral gyrus medial segment	73 ± 14	51 ± 12	<0.0001
Superior frontal gyrus medial segment	95 ± 16	73 ± 14	<0.0001
Opercular part of the inferior frontal gyrus	92 ± 15	72 ± 15	<0.0001
Orbital part of the inferior frontal gyrus	88 ± 14	72 ± 14	0.0002
Posterior orbital gyrus	88 ± 11	71 ± 13	<0.0001
Precentral gyrus	71 ± 13	52 ± 12	<0.0001
Superior frontal gyrus	78 ± 16	57 ± 14	<0.0001
Supplementary motor cortex	88 ± 15	65 ± 13	<0.0001
Triangular part of the inferior frontal gyrus	92 ± 16	73 ± 14	<0.0001
Temporal lobe			
Hippocampus	64 ± 9	47 ± 8	<0.0001
Anterior insula	80 ± 10	66 ± 12	<0.0001
Central operculum	80 ± 11	65 ± 12	<0.0001
Entorhinal area	57 ± 8	44 ± 8	<0.0001
Fusiform gyrus	62 ± 10	43 ± 10	<0.0001
Inferior temporal gyrus	69 ± 13	47 ± 12	<0.0001
Middle temporal gyrus	83 ± 14	60 ± 13	<0.0001
Parahippocampal gyrus	58 ± 9	43 ± 8	<0.0001
Posterior insula	76 ± 10	62 ± 11	<0.0001
Planum polare	79 ± 10	65 ± 11	<0.0001
Planum temporale	87 ± 12	69 ± 13	<0.0001
Superior temporal gyrus	83 ± 12	62 ± 12	<0.0001
Temporal pole	67 ± 10	51 ± 12	<0.0001
Transverse temporal gyrus	88 ± 11	72 ± 13	<0.0001
Parietal lobe			
Angular gyrus	83 ± 15	58 ± 14	<0.0001
Central operculum	80 ± 11	65 ± 12	<0.0001
Postcentral gyrus medial segment	65 ± 14	44 ± 12	<0.0001
Precuneus	79 ± 16	52 ± 12	<0.0001
Parietal operculum	82 ± 12	65 ± 12	<0.0001
Postcentral gyrus	64 ± 12	45 ± 11	<0.0001
Supramarginal gyrus	83 ± 14	60 ± 13	<0.0001
Superior parietal lobule	62 ± 14	40 ± 12	<0.0001
Occipital lobe			
Calcarine cortex	71 ± 13	47 ± 11	<0.0001
Cuneus	73 ± 15	47 ± 13	<0.0001
Fusiform gyrus	62 ± 10	43 ± 10	<0.0001
Inferior occipital gyrus	69 ± 14	46 ± 14	<0.0001
Lingual gyrus	67 ± 12	46 ± 12	<0.0001
Middle occipital gyrus	75 ± 15	52 ± 14	<0.0001
Occipital pole	71 ± 15	43 ± 14	<0.0001
Occipital fusiform gyrus	62 ± 11	42 ± 13	<0.0001
Superior occipital gyrus	62 ± 13	41 ± 13	<0.0001

Values are means ± SD. Perfusion is reported (in mL/100 g/min) via pseudocontinuous arterial spin labeling (pcASL) and T1 magnetic resonancer imaging (MRI) scans. Regional analysis by computational analysis toolbox (CAT, v.12). Regions normalized to Montreal Neurological Institute (MNI).

Present mean gray and white matter perfusion levels for both sexes were higher than most previously reported CBF values, and the magnitude of the difference between sexes was higher compared with several previous studies (14, 16, 21, 64) but similar to one study (65), which had a more comparable age population and similar exclusion criteria, suggesting even middle age is linked to reduced perfusion. The higher CBF values of the present data may be a product of the relatively young age of the study population. Age is associated with reduced cerebral blood flow (14, 21, 66) as well as reduced rate of oxygen consumption by the brain [cerebral metabolic rate of oxygen (CMR_{O_2})], which is directly associated with CBF (66). In addition, females show a steeper slope of CBF decline with age, suggesting the sex differences are attenuated in older age (14). Consistent with this idea, all of the previously mentioned studies that reported lower CBF values assessed sex differences in groups with large age ranges (14, 16, 21, 64), and data in Fig. 2 and Table 2 suggest that sex differences in CBF are actually larger when age is limited to adults between 18 and 30 yr old.

Because gray matter (GM) exhibits higher perfusion than white matter (WM), larger gray matter volume in females could explain higher relative total brain blood flow in females; however, present results indicate no sex differences in the whole brain GM/WM ratio. Previous studies indicate females exhibit a higher percentage of gray matter (40) and the GM/WM ratio was higher compared with males (38). However, their results may be due to the hormonal impacts, such as menstrual cycle and oral contraception, on gray matter volume (38, 67, 68). Numerous regional gray matter volumes are significantly lower in naturally cycling females when compared with females on oral contraceptives (67). Therefore, the exclusion of females using oral contraceptives may decrease the observed GM/WM differences. Additionally, high aerobic fitness is associated with greater gray matter volumes in young and older adults (69–71), so alterations in fitness may impact volumetric outcomes. The present study collected relative peak oxygen

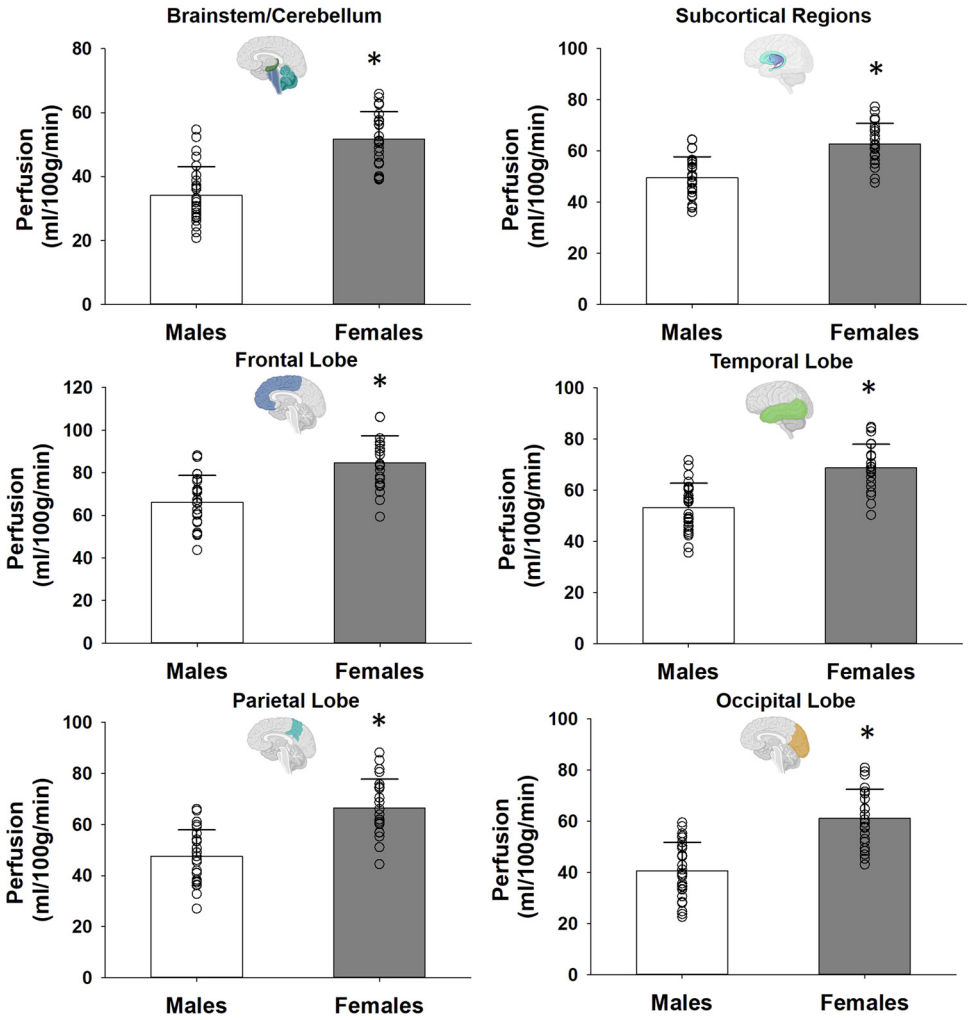

Figure 3. Perfusion of the lobes and anatomical regions for males ($n = 26$) and females ($n = 22$). *$P < 0.05$, significant difference between males and females, using Shaffer's sequential method.

consumption ($\dot{V}O_{2peak}$) from 32 subjects (females, $n = 12$, $\dot{V}O_{2peak} = 43 \pm 8$ mL/kg/min; males, $n = 20$, $\dot{V}O_{2peak} = 53 \pm 10$ mL/kg/min) using a graded treadmill test. Based on the American College of Sports Medicine's (ACSM) fitness categories, the average of both sexes is of moderate to high fitness (females, 75th percentile, males, 85th percentile), suggesting a range of cardiorespiratory fitness is unlikely to heavily influence the present sex differences of GM/WM ratios and subsequently in CBF.

Limiting study visits in females to menstrual cycle to *days 1–7* was aimed to minimize sex steroid differences between men and women, allowing a better understanding of sex differences per se in controlling CBF. Specifically, dehydroepiandrosterone sulfate (DHEAS) is found in both sexes but typically is greater in males, and DHEAS is negatively correlated with cerebral perfusion (16). Testosterone is negatively correlated with CBF in females but not in males (16). Additionally, estrogen receptors in the cerebral vasculature modulate the synthesis and release of endothelial-derived vasodilators [such as endothelial-derived nitrogen oxide synthase (eNOS) (72)], which may increase vasodilation (73). In support of this, Doppler studies assessing the carotid arteries suggest estrogen is associated with decreased cerebrovascular resistance (74, 75), but studies assessing cerebral perfusion conclude estrogen is not significantly correlated (16) or weakly correlated (76) with CBF. Alternatively, there is a strong negative correlation between progesterone and CBF in young, healthy females (76). However, higher MCA velocity is seen during the luteal phase when progesterone and estrogen are both elevated (16, 20, 29). The present study design was aimed at minimizing sex hormone differences while still highlighting fundamental sex differences in CBF, consistent with the concept that nonhormonal mechanisms may be more influential on sex differences in CBF.

Two other factors known to influence CBF are arterial CO_2 and blood pressure, which were assessed as $ETCO_2$ and MAP, respectively (Supplemental Table S1). Females exhibited 3 mmHg lower resting $ETCO_2$ on average than males (Table 3). Since increasing $ETCO_2$ is positively correlated with CBF (77, 78), a lower $ETCO_2$ in females may slightly underestimate sex differences in CBF. Similarly, lower MAP in females (Table 3) would be expected to drive lower perfusion. When accounting for MAP [cerebrovascular conductance (CVC)], CVC exhibited an even larger relative sex difference than CBF (Supplemental Table S2). In sum, the current sex differences between $ETCO_2$ and MAP may slightly underestimate the observed sex differences in cerebral vasodilation.

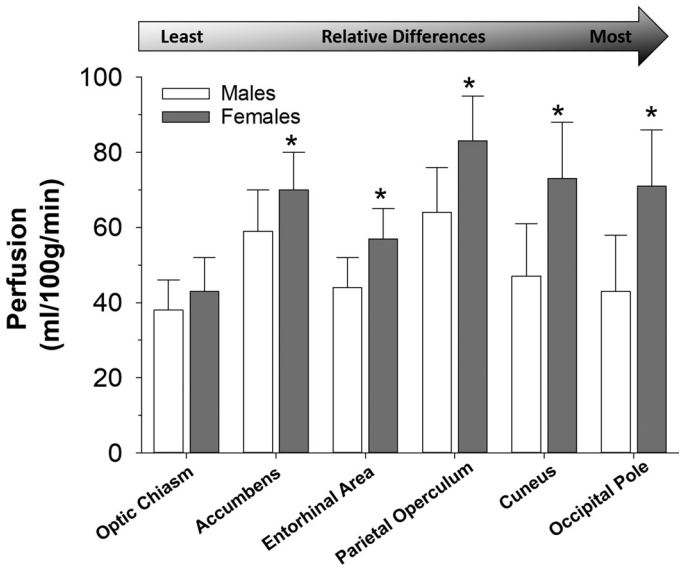

Figure 4. Representative selections highlighting the range in differences between sexes in regional perfusion. Regions selected depict the least different (*left*) to most different (*right*) based on relative sex difference. Optic chiasm (14%), accumbens (19%), entorhinal area (29%), parietal operculum (28%), cuneus (55%), and occipital pole (66%). See Table 3 for the complete regional analysis for males ($n = 26$) and females ($n = 22$). *$P < 0.05$, significant difference between female and male participants, using Shaffer's sequential method.

Metabolic activity and oxygen-carrying capacity could impact sex differences in CBF as increases in CMR_{O_2} are associated with increases in CBF (79). However, previously, no sex differences have been found in CMR_{O_2} (64, 80, 81). If CMR_{O_2} is similar between sexes, then differences in oxygen-carrying capacity could account for sex differences in CBF. In this study, males had significantly higher hemoglobin than females, and hemoglobin was negatively correlated with CBF ($r = -0.68$; $P < 0.001$). Females exhibit lower arterial oxygen content (Ca_{O_2}) but higher CDo_2 in both gray and white matter (Supplemental Table S3). Therefore, present data support the concept that higher CBF in females may be necessary to achieve similar CMR_{O_2}, presuming similar O_2 diffusion.

Several previsit procedures and exclusion criteria may affect perfusion. To limit these potential impacts, our study design included withholding caffeine to avoid reduced CBF, sometimes by as much as 27% (82, 83). Previous work indicates meal ingestion (84) or insulin infusions (85) can alter perfusion, so a minimum of 8 h of fasting was employed. Using medical history questionnaires, this study excluded subjects who experienced many medical conditions/diseases that may have directly impacted cerebral blood flow or indirectly via cardiovascular influences. First, we excluded subjects who had a history of cardiovascular risk factors such as hypertension, obesity, diabetes, smoking, elevated BMI, and high blood concentrations of lipids and glucose since all of these are linked to cardiovascular disease, which might directly or indirectly impact CBF. Second, since several sex-predominant brain disorders are linked to CBF alterations, we excluded subjects with self-reported depression and anxiety as well as cardiovascular, inflammatory, and neurological disorders. CBF is reduced in depression (5), smoking (27), hypertension (86), diabetes (25), obesity (87), and hyperlipidemia (88). Therefore, the striking sex differences in perfusion observed presently are likely not influenced by these conditions or comorbidities.

Mechanistic Insight

This study did not test specific mechanisms, which may explain these large sex differences. The literature provides many promising directions, although some are challenging to test in humans because of safety considerations. Nitric oxide is not a likely candidate as recent work suggests NOS inhibition only reduces CBF by 4%–10% (89, 90). Cyclooxygenase inhibition can markedly reduce resting CBF in healthy adults and our prior transcranial Doppler (TCD) work indicates no sex differences in basal CBF (91), although indomethacin did abolish higher CBF during late follicular phase compared with early phase of menstrual cycle (20), but this difference would not explain current findings. Importantly, the tightly controlled experimental variables discussed above also provide strong evidence for mechanisms that do not explain sex differences, which allows future research to focus on other promising avenues.

Physiological versus Clinical Relevance

Physiologically, the higher CBF in females appears necessary to meet O_2 delivery demands (Supplemental Table S2). On the other hand, the full clinical relevance of our findings remains unclear. A reasonable hypothesis is higher CBF serves as a protective mechanism, given the relationships between lower/reduced CBF and poor brain outcomes including dementia and Alzheimer's disease (92). In particular, the risk of these conditions generally increases as CBF declines, and risk appears lower in women at least until menopause when sex differences in CBF tend to be reduced.

Limitations

Present findings may not directly translate to ~25% of the American female population (aged 18–44 yr old) who report using hormonal contraception (93). Similarly, we chose to study females during the early follicular menstrual phase, so our results do not test the important question of how CBF changes over the menstrual cycle). Sex hormones analysis was not performed, but given cycle tracking, it is likely blood hormone levels would be similar to other studies comparing males to females in the early follicular phase with the goal of minimizing sex hormone differences (16, 20). Insight on CBF from a full hormone data set may be limited as previous studies show relatively weak correlations between sex hormone levels and CBF (16, 20, 76).

Another potential factor influencing female CBF relates to parity, time since last pregnancy, or if any pregnancies included a history of preeclampsia or gestational diabetes as these conditions may increase cardiovascular disease risk (94). Additionally, some female subjects may have taken oral contraceptives for some unknown amount of time 6 mo before starting the study. We did not collect this information and therefore cannot rule out their unknown influence on the present data.

We did not control the time of day in which scans were taken, which has been suggested to influence resting CBF (95). However, a Pearson correlation showed no significance between time of day and CBF in gray matter (females, $r = -0.10$, $P = 0.66$; males, $r = 0.16$, $P = 0.43$) or white matter (females, $r = -0.06$, $P = 0.79$; males, $r = 0.26$, $P = 0.20$) in either sex. A recent study using TCD indicates basal MCA velocity also does not vary diurnally (96).

Conclusions

This study presents detailed MRI analyses and rigorous experimental controls, highlighting substantial fundamental sex differences in global and regional cerebral blood flow in 18- to 30-yr-old adults. These data confirm prior MRI brain studies of greater perfusion in females and extend the conceptual framework by separating gray from white matter and delineating a wide range of sex differences in dozens of brain regions. Females exhibited ~40% higher CBF globally and in gray and white matter, ranging from 14% to 66% in the 67 of the 68 brain regions studied. Likely due to the young age and strict exclusion criteria, the CBF values collected in this study were higher than other previous studies that included wider age ranges and did not limit confounding factors. Because healthy blood flow in young adults is so markedly different between the sexes, future research in this area is necessary to uncover the mechanisms behind the sex difference. In the context of the exclusion criteria employed here, these data may serve as a robust baseline for future comparisons exploring the impacts of menstrual cycle, contraception, and the systematic addition of aging and confounders like obesity, hypertension, etc., which may aid in the development of diagnostic and therapeutic tools to treat complex sex-specific brain pathologies.

DATA AVAILABILITY

Data will be made available upon reasonable request, upon ethical approval for data sharing.

SUPPLEMENTAL MATERIAL

Supplemental Tables S1–S3: https://doi.org/10.6084/m9.figshare.26383753.

GRANTS

This work was funded by National Heart, Lung, and Blood Institute Grant 5R01HL150361-04 (to J.D.M., K.D.D., B.M.W., S.S., H.K.M., N.F.B., M.W.E., O.W., and W.G.S.) and Baylor College of Medicine Grants TRISH P0603 and 7000001428 (to K.D.D.).

DISCLOSURES

No conflicts of interest, financial or otherwise, are declared by the authors.

AUTHOR CONTRIBUTIONS

R.C.S., O.W., and W.G.S. conceived and designed research; J.D.M., O.W., W.G.S., K.D.D., B.M.W., S.S., H.K.M., and T.L.H. performed experiments; J.D.M., K.D.D., B.M.W., H.K.M., K.J.C., and N.F.B. analyzed data; J.D.M., R.C.S., O.W., W.G.S., K.D.D., and N.F.B. interpreted results of experiments; K.D.D. prepared figures; J.D.M., O.W., and W.G.S. drafted manuscript; J.D.M., R.C.S., O.W., W.G.S., K.D.D., B.M.W., H.K.M., T.L.H., K.J.C., N.F.B., and M.W.E. edited and revised manuscript; J.D.M., O.W., W.G.S., K.D.D., and B.M.W. approved final version of manuscript.

REFERENCES

1. **Alexopoulos P**, **Sorg C**, **Forschler A**, **Grimmer T**, **Skokou M**, **Wohlschlager A**, **Perneczky R**, **Zimmer C**, **Kurz A**, **Preibisch C.** Perfusion abnormalities in mild cognitive impairment and mild dementia in Alzheimer's disease measured by pulsed arterial spin labeling MRI. *Eur Arch Psychiatry Clin Neurosci* 262: 69–77, 2012. doi:10.1007/s00406-011-0226-2.
2. **Detre JA**, **Alsop DC**, **Vives LR**, **Maccotta L**, **Teener JW**, **Raps EC.** Noninvasive MRI evaluation of cerebral blood flow in cerebrovascular disease. *Neurology* 50: 633–641, 1998. doi:10.1212/wnl.50.3.633.
3. **Iadecola C.** Neurovascular regulation in the normal brain and in Alzheimer's disease. *Nat Rev Neurosci* 5: 347–360, 2004. doi:10.1038/nrn1387.
4. **Toyoda K**, **Minematsu K**, **Yamaguchi T.** Long-term changes in cerebral blood flow according to different types of ischemic stroke. *J Neurol Sci* 121: 222–228, 1994. doi:10.1016/0022-510x(94)90356-5.
5. **Ritter C**, **Buchmann A**, **Muller ST**, **Hersberger M**, **Haynes M**, **Ghisleni C**, **Tuura R**, **Hasler G.** Cerebral perfusion in depression: relationship to sex, dehydroepiandrosterone sulfate and depression severity. *Neuroimage Clin* 32: 102840, 2021. doi:10.1016/j.nicl.2021.102840.
6. **Rossi MF**, **Tumminello A**, **Marconi M**, **Gualano MR**, **Santoro PE**, **Malorni W**, **Moscato U.** Sex and gender differences in migraines: a narrative review. *Neurol Sci* 43: 5729–5734, 2022. doi:10.1007/s10072-022-06178-6.
7. **Reckelhoff JF.** Gender differences in the regulation of blood pressure. *Hypertension* 37: 1199–1208, 2001. doi:10.1161/01.hyp.37.5.1199.
8. **Hajjar I**, **Quach L**, **Yang F**, **Chaves PH**, **Newman AB**, **Mukamal K**, **Longstreth W, Jr**,**Inzitari M**, **Lipsitz LA.** Hypertension, white matter hyperintensities, and concurrent impairments in mobility, cognition, and mood: the Cardiovascular Health Study. *Circulation* 123: 858–865, 2011. doi:10.1161/CIRCULATIONAHA.110.978114.
9. **Macey PM**, **Kumar R**, **Yan-Go FL**, **Woo MA**, **Harper RM.** Sex differences in white matter alterations accompanying obstructive sleep apnea. *Sleep* 35: 1603–1613, 2012. doi:10.5665/sleep.2228.
10. **Netzer N**, **Werner P**, **Jochums I**, **Lehmann M**, **Strohl KP.** Blood flow of the middle cerebral artery with sleep-disordered breathing: correlation with obstructive hypopneas. *Stroke* 29: 87–93, 1998. doi:10.1161/01.str.29.1.87.
11. **Li X**, **Zhou W**, **Yi Z.** A glimpse of gender differences in schizophrenia. *Gen Psychiatr* 35: e100823, 2022. doi:10.1136/gpsych-2022-100823.
12. **Gur RE**, **Gur RC.** Gender differences in regional cerebral blood flow. *Schizophr Bull* 16: 247–254, 1990. doi:10.1093/schbul/16.2.247.
13. **Xu L**, **Qin W**, **Zhuo C**, **Liu H**, **Zhu J**, **Yu C.** Combination of volume and perfusion parameters reveals different types of grey matter changes in schizophrenia. *Sci Rep* 7: 435, 2017. doi:10.1038/s41598-017-00352-z.
14. **Alisch JS**, **Khattar N**, **Kim RW**, **Cortina LE**, **Rejimon AC**, **Qian W**, **Ferrucci L**, **Resnick SM**, **Spencer RG**, **Bouhrara M.** Sex and age-related differences in cerebral blood flow investigated using pseudo-continuous arterial spin labeling magnetic resonance imaging. *Aging (Albany NY)* 13: 4911–4925, 2021. doi:10.18632/aging.202673.
15. **Esposito G**, **Van Horn JD**, **Weinberger DR**, **Berman KF.** Gender differences in cerebral blood flow as a function of cognitive state with PET. *J Nucl Med* 37: 559–564, 1996.
16. **Ghisleni C**, **Bollmann S**, **Biason-Lauber A**, **Poil SS**, **Brandeis D**, **Martin E**, **Michels L**, **Hersberger M**, **Suckling J**, **Klaver P**, **O'Gorman RL.** Effects of steroid hormones on sex differences in cerebral perfusion. *PLoS One* 10: e0135827, 2015. doi:10.1371/journal.pone.0135827.
17. **Liu R**, **Sui X**, **Laditka JN**, **Church TS**, **Colabianchi N**, **Hussey J**, **Blair SN.** Cardiorespiratory fitness as a predictor of dementia mortality in men and women. *Med Sci Sports Exerc* 44: 253–259, 2012. doi:10.1249/MSS.0b013e31822cf717.

18. **Mathew RJ**, **Wilson WH**, **Tant SR.** Determinants of resting regional cerebral blood flow in normal subjects. *Biol Psychiatry* 21: 907–914, 1986. doi:10.1016/0006-3223(86)90264-7.
19. **Rodriguez G**, **Warkentin S**, **Risberg J**, **Rosadini G.** Sex differences in regional cerebral blood flow. *J Cereb Blood Flow Metab* 8: 783–789, 1988. doi:10.1038/jcbfm.1988.133.
20. **Peltonen GL**, **Harrell JW**, **Aleckson BP**, **LaPlante KM**, **Crain MK**, **Schrage WG.** Cerebral blood flow regulation in women across menstrual phase: differential contribution of cyclooxygenase to basal, hypoxic, and hypercapnic vascular tone. *Am J Physiol Regul Integr Comp Physiol* 311: R222–R231, 2016. doi:10.1152/ajpregu.00106.2016.
21. **Juttukonda MR**, **Li B**, **Almaktoum R**, **Stephens KA**, **Yochim KM**, **Yacoub E**, **Buckner RL**, **Salat DH.** Characterizing cerebral hemodynamics across the adult lifespan with arterial spin labeling MRI data from the Human Connectome Project-Aging. *Neuroimage* 230: 117807, 2021. doi:10.1016/j.neuroimage.2021.117807.
22. **van Dalen JW**, **Mutsaerts H**, **Nederveen AJ**, **Vrenken H**, **Steenwijk MD**, **Caan MW**, **Majoie C**, **van Gool WA**, **Richard E.** white matter hyperintensity volume and cerebral perfusion in older individuals with hypertension using arterial spin-labeling. *AJNR Am J Neuroradiol* 37: 1824–1830, 2016. doi:10.3174/ajnr.A4828.
23. **Knight SP**, **Laird E**, **Williamson W**, **O'Connor J**, **Newman L**, **Carey D**, **De Looze C**, **Fagan AJ**, **Chappell MA**, **Meaney JF**, **Kenny RA.** Obesity is associated with reduced cerebral blood flow – modified by physical activity. *Neurobiol Aging* 105: 35–47, 2021. doi:10.1016/j.neurobiolaging.2021.04.008.
24. **Selim M**, **Jones R**, **Novak P**, **Zhao P**, **Novak V.** The effects of body mass index on cerebral blood flow velocity. *Clin Auton Res* 18: 331–338, 2008. doi:10.1007/s10286-008-0490-z.
25. **Chau AC**, **Cheung EY**, **Chan KH**, **Chow WS**, **Shea YF**, **Chiu PK**, **Mak HK.** Impaired cerebral blood flow in type 2 diabetes mellitus - a comparative study with subjective cognitive decline, vascular dementia and Alzheimer's disease subjects. *Neuroimage Clin* 27: 102302, 2020. doi:10.1016/j.nicl.2020.102302.
26. **Smit RA**, **Trompet S**, **Sabayan B**, **Le Cessie S**, **van der Grond J**, **van Buchem MA**, **de Craen AJ**, **Jukema JW.** Higher visit-to-visit low-density lipoprotein cholesterol variability is associated with lower cognitive performance, lower cerebral blood flow, and greater white matter hyperintensity load in older subjects. *Circulation* 134: 212–221, 2016. doi:10.1161/CIRCULATIONAHA.115.020627.
27. **Song Y**, **Kim JG**, **Cho HJ**, **Kim JK**, **Suh DC.** Evaluation of cerebral blood flow change after cigarette smoking using quantitative MRA. *PLoS One* 12: e0184551, 2017. doi:10.1371/journal.pone.0184551.
28. **Otomo M**, **Harada M**, **Abe T**, **Matsumoto Y**, **Abe Y**, **Kanazawa Y**, **Miyoshi M**, **Kabasawa H**, **Takahashi Y.** Reproducibility and variability of quantitative cerebral blood flow measured by multi-delay 3D arterial spin labeling according to sex and menstrual cycle. *J Med Invest* 67: 321–327, 2020. doi:10.2152/jmi.67.321.
29. **Brackley KJ**, **Ramsay MM**, **Broughton Pipkin F**, **Rubin PC.** The effect of the menstrual cycle on human cerebral blood flow: studies using Doppler ultrasound. *Ultrasound Obstet Gynecol* 14: 52–57, 1999. doi:10.1046/j.1469-0705.1999.14010052.x.
30. **Liu Y**, **Zhu X**, **Feinberg D**, **Guenther M**, **Gregori J**, **Weiner MW**, **Schuff N.** Arterial spin labeling MRI study of age and gender effects on brain perfusion hemodynamics. *Magn Reson Med* 68: 912–922, 2012. doi:10.1002/mrm.23286.
31. **Reinberg AE**, **Touitou Y**, **Soudant E**, **Bernard D**, **Bazin R**, **Mechkouri M.** Oral contraceptives alter circadian rhythm parameters of cortisol, melatonin, blood pressure, heart rate, skin blood flow, transepidermal water loss, and skin amino acids of healthy young women. *Chronobiol Int* 13: 199–211, 1996. doi:10.3109/07420529609012653.
32. **Turner CG**, **Stanhewicz AE**, **Nielsen KE**, **Otis JS**, **Feresin RG**, **Wong BJ.** Effects of biological sex and oral contraceptive pill use on cutaneous microvascular endothelial function and nitric oxide-dependent vasodilation in humans. *J Appl Physiol (1985)* 134: 858–867, 2023. doi:10.1152/japplphysiol.00586.2022.
33. **Houghton BL**, **Holowatz LA**, **Minson CT.** Influence of progestin bioactivity on cutaneous vascular responses to passive heating. *Med Sci Sports Exerc* 37: 45–51, 2005. doi:10.1249/01.mss.0000150075.81511.fe.
34. **Limberg JK**, **Peltonen GL**, **Johansson RE**, **Harrell JW**, **Kellawan JM**, **Eldridge MW**, **Sebranek JJ**, **Walker BJ**, **Schrage WG.** Greater beta-adrenergic receptor mediated vasodilation in women using oral contraceptives. *Front Physiol* 7: 215, 2016. doi:10.3389/fphys.2016.00215.
35. **Liu JX**, **Min LZ**, **Liu RD**, **Zhang XY**, **Wu MT**, **Di Q**, **Ma XD.** The effect of exercise on cerebral blood flow and executive function among young adults: a double-blinded randomized controlled trial. *Sci Rep* 13: 8269, 2023. doi:10.1038/s41598-023-33063-9.
36. **Murrell CJ**, **Cotter JD**, **Thomas KN**, **Lucas SJ**, **Williams MJ**, **Ainslie PN.** Cerebral blood flow and cerebrovascular reactivity at rest and during sub-maximal exercise: effect of age and 12-week exercise training. *Age (Dordr)* 35: 905–920, 2013. doi:10.1007/s11357-012-9414-x.
37. **Parkes LM**, **Rashid W**, **Chard DT**, **Tofts PS.** Normal cerebral perfusion measurements using arterial spin labeling: reproducibility, stability, and age and gender effects. *Magn Reson Med* 51: 736–743, 2004. doi:10.1002/mrm.20023.
38. **Witte AV**, **Savli M**, **Holik A**, **Kasper S**, **Lanzenberger R.** Regional sex differences in grey matter volume are associated with sex hormones in the young adult human brain. *Neuroimage* 49: 1205–1212, 2010. doi:10.1016/j.neuroimage.2009.09.046.
39. **Chen X**, **Sachdev PS**, **Wen W**, **Anstey KJ.** Sex differences in regional gray matter in healthy individuals aged 44-48 years: a voxel-based morphometric study. *Neuroimage* 36: 691–699, 2007. doi:10.1016/j.neuroimage.2007.03.063.
40. **Gur RC**, **Turetsky BI**, **Matsui M**, **Yan M**, **Bilker W**, **Hughett P**, **Gur RE.** Sex differences in brain gray and white matter in healthy young adults: correlations with cognitive performance. *J Neurosci* 19: 4065–4072, 1999. doi:10.1523/JNEUROSCI.19-10-04065.1999.
41. **Alwatban MR**, **Aaron SE**, **Kaufman CS**, **Barnes JN**, **Brassard P**, **Ward JL**, **Miller KB**, **Howery AJ**, **Labrecque L**, **Billinger SA.** Effects of age and sex on middle cerebral artery blood velocity and flow pulsatility index across the adult lifespan. *J Appl Physiol (1985)* 130: 1675–1683, 2021. doi:10.1152/japplphysiol.00926.2020.
42. **Kellawan JM**, **Harrell JW**, **Roldan-Alzate A**, **Wieben O**, **Schrage WG.** Regional hypoxic cerebral vasodilation facilitated by diameter changes primarily in anterior versus posterior circulation. *J Cereb Blood Flow Metab* 37: 2025–2034, 2017. doi:10.1177/0271678X16659497.
43. **Kellawan JM**, **Peltonen GL**, **Harrell JW**, **Roldan-Alzate A**, **Wieben O**, **Schrage WG.** Differential contribution of cyclooxygenase to basal cerebral blood flow and hypoxic cerebral vasodilation. *Am J Physiol Regul Integr Comp Physiol* 318: R468–R479, 2020. doi:10.1152/ajpregu.00132.2019.
44. **Harrell JW**, **Schrage WG.** Cyclooxygenase-derived vasoconstriction restrains hypoxia-mediated cerebral vasodilation in young adults with metabolic syndrome. *Am J Physiol Heart Circ Physiol* 306: H261–H269, 2014. doi:10.1152/ajpheart.00709.2013.
45. **Harrell JW**, **Peltonen GL**, **Schrage WG.** Reactive oxygen species and cyclooxygenase products explain the majority of hypoxic cerebral vasodilation in healthy humans. *Acta Physiol (Oxf)* 226: e13288, 2019. doi:10.1111/apha.13288.
46. **Alsop DC**, **Casement M**, **de Bazelaire C**, **Fong T**, **Press DZ.** Hippocampal hyperperfusion in Alzheimer's disease. *Neuroimage* 42: 1267–1274, 2008. doi:10.1016/j.neuroimage.2008.06.006.
47. **Wierenga CE**, **Clark LR**, **Dev SI**, **Shin DD**, **Jurick SM**, **Rissman RA**, **Liu TT**, **Bondi MW.** Interaction of age and APOE genotype on cerebral blood flow at rest. *J Alzheimers Dis* 34: 921–935, 2013. doi:10.3233/JAD-121897.
48. **Fleisher AS**, **Podraza KM**, **Bangen KJ**, **Taylor C**, **Sherzai A**, **Sidhar K**, **Liu TT**, **Dale AM**, **Buxton RB.** Cerebral perfusion and oxygenation differences in Alzheimer's disease risk. *Neurobiol Aging* 30: 1737–1748, 2009. doi:10.1016/j.neurobiolaging.2008.01.012.
49. **Liotti M**, **Mayberg HS**, **McGinnis S**, **Brannan SL**, **Jerabek P.** Unmasking disease-specific cerebral blood flow abnormalities: mood challenge in patients with remitted unipolar depression. *Am J Psychiatry* 159: 1830–1840, 2002. doi:10.1176/appi.ajp.159.11.1830.
50. **Hasler G**, **Fromm S**, **Alvarez RP**, **Luckenbaugh DA**, **Drevets WC**, **Grillon C.** Cerebral blood flow in immediate and sustained anxiety. *J Neurosci* 27: 6313–6319, 2007. doi:10.1523/JNEUROSCI.5369-06.2007.
51. **Papadaki E**, **Kavroulakis E**, **Bertsias G**, **Fanouriakis A**, **Karageorgou D**, **Sidiropoulos P**, **Papastefanakis E**, **Boumpas DT**, **Simos P.** Regional

cerebral perfusion correlates with anxiety in neuropsychiatric SLE: evidence for a mechanism distinct from depression. *Lupus* 28: 1678–1689, 2019. doi:10.1177/0961203319887793.
52. **Gu T**, **Korosec FR**, **Block WF**, **Fain SB**, **Turk Q**, **Lum D**, **Zhou Y**, **Grist TM**, **Haughton V**, **Mistretta CA.** PC VIPR: a high-speed 3D phase-contrast method for flow quantification and high-resolution angiography. *AJNR Am J Neuroradiol* 26: 743–749, 2005.
53. **Johnson KM**, **Lum DP**, **Turski PA**, **Block WF**, **Mistretta CA**, **Wieben O.** Improved 3D phase contrast MRI with off-resonance corrected dual echo VIPR. *Magn Reson Med* 60: 1329–1336, 2008. doi:10.1002/mrm.21763.
54. **Schrauben E**, **Wahlin A**, **Ambarki K**, **Spaak E**, **Malm J**, **Wieben O**, **Eklund A.** Fast 4D flow MRI intracranial segmentation and quantification in tortuous arteries. *J Magn Reson Imaging* 42: 1458–1464, 2015. doi:10.1002/jmri.24900.
55. **Vikner T**, **Nyberg L**, **Holmgren M**, **Malm J**, **Eklund A**, **Wahlin A.** Characterizing pulsatility in distal cerebral arteries using 4D flow MRI. *J Cereb Blood Flow Metab* 40: 2429–2440, 2020. doi:10.1177/0271678X19886667.
56. **Rivera-Rivera LA**, **Turski P**, **Johnson KM**, **Hoffman C**, **Berman SE**, **Kilgas P**, **Rowley HA**, **Carlsson CM**, **Johnson SC**, **Wieben O.** 4D flow MRI for intracranial hemodynamics assessment in Alzheimer's disease. *J Cereb Blood Flow Metab* 36: 1718–1730, 2016. doi:10.1177/0271678X15617171.
57. **Hoscheidt SM**, **Kellawan JM**, **Berman SE**, **Rivera-Rivera LA**, **Krause RA**, **Oh JM**, **Beeri MS**, **Rowley HA**, **Wieben O**, **Carlsson CM**, **Asthana S**, **Johnson SC**, **Schrage WG**, **Bendlin BB.** Insulin resistance is associated with lower arterial blood flow and reduced cortical perfusion in cognitively asymptomatic middle-aged adults. *J Cereb Blood Flow Metab* 37: 2249–2261, 2017. doi:10.1177/0271678X16663214.
58. **Liu TT.** Neurovascular factors in resting-state functional MRI. *Neuroimage* 80: 339–348, 2013. doi:10.1016/j.neuroimage.2013.04.071.
59. **Gaser C**, **Dahnke F**, **Kurth K**, **Luders E**, **The Alzheimer's Disease Neuroimaging Initiative.** Alzheimer's disease neuroimaging initiative. a computational anatomy toolbox for the analysis of structural MRI Data. *Gigascience* 13: giae049, 2024. doi:10.1093/gigascience/giae049.
60. **Bouthillier A**, **van Loveren HR**, **Keller JT.** Segments of the internal carotid artery: a new classification. *Neurosurgery* 38: 425–432, 1996. doi:10.1097/00006123-199603000-00001.
61. **Mcintosh R**, **Anderson V.** A comprehensive tissue properties database provided for the thermal assessment of a human at rest. *Biophys Rev Lett* 5: 129–151, 2010. doi:10.1142/S1793048010001184.
62. **Levin JR**, **Serlin RC**, **Seaman MA.** A controlled, powerful multiple-comparison strategy for several situations. *Psychol Bull* 115: 153–159, 1994. doi:10.1037//0033-2909.115.1.153.
63. **Shaffer JP.** Modified sequentially rejective multiple test procedures. *J Am Stat Assoc* 81: 826–831, 1986. doi:10.2307/2289016.
64. **Aanerud J**, **Borghammer P**, **Rodell A**, **Jonsdottir KY**, **Gjedde A.** Sex differences of human cortical blood flow and energy metabolism. *J Cereb Blood Flow Metab* 37: 2433–2440, 2017. doi:10.1177/0271678X16668536.
65. **Chen CM**, **Yang HC**, **Hsieh HH**, **Liao TY**, **Huang YC**, **Peng SL.** Characterization of regional differences in cerebral vascular response to breath holding using BOLD fMRI. *Int J Imaging Syst Tech* 31: 180–188, 2020. doi:10.1002/ima.22473.
66. **De Vis JB**, **Hendrikse J**, **Bhogal A**, **Adams A**, **Kappelle LJ**, **Petersen ET.** Age-related changes in brain hemodynamics; a calibrated MRI study. *Hum Brain Mapp* 36: 3973–3987, 2015. doi:10.1002/hbm.22891.
67. **Pletzer B**, **Kronbichler M**, **Aichhorn M**, **Bergmann J**, **Ladurner G**, **Kerschbaum HH.** Menstrual cycle and hormonal contraceptive use modulate human brain structure. *Brain Res* 1348: 55–62, 2010. doi:10.1016/j.brainres.2010.06.019.
68. **Chen KX**, **Worley S**, **Foster H**, **Edasery D**, **Roknsharifi S**, **Ifrah C**, **Lipton ML.** Oral contraceptive use is associated with smaller hypothalamic and pituitary gland volumes in healthy women: a structural MRI study. *PLoS One* 16: e0249482, 2021. doi:10.1371/journal.pone.0249482.
69. **Liu Y**, **Zhu L**, **Cai K**, **Dong X**, **Xiong X**, **Liu Z**, **Chen A.** Relationship between cardiorespiratory fitness and executive function in young adults: mediating effects of gray matter volume. *Brain Sci* 12: 1441, 2022. doi:10.3390/brainsci12111441.
70. **Erickson KI**, **Leckie RL**, **Weinstein AM.** Physical activity, fitness, and gray matter volume. *Neurobiol Aging* 35, *Suppl* 2: S20–28, 2014. doi:10.1016/j.neurobiolaging.2014.03.034.
71. **Erickson KI**, **Prakash RS**, **Voss MW**, **Chaddock L**, **Hu L**, **Morris KS**, **White SM**, **Wojcicki TR**, **McAuley E**, **Kramer AF.** Aerobic fitness is associated with hippocampal volume in elderly humans. *Hippocampus* 19: 1030–1039, 2009. doi:10.1002/hipo.20547.
72. **McNeill AM**, **Zhang C**, **Stanczyk FZ**, **Duckles SP**, **Krause DN.** Estrogen increases endothelial nitric oxide synthase via estrogen receptors in rat cerebral blood vessels: effect preserved after concurrent treatment with medroxyprogesterone acetate or progesterone. *Stroke* 33: 1685–1691, 2002. doi:10.1161/01.str.0000016325.54374.93.
73. **Stirone C**, **Duckles SP**, **Krause DN.** Multiple forms of estrogen receptor-alpha in cerebral blood vessels: regulation by estrogen. *Am J Physiol Endocrinol Metab* 284: E184–E192, 2003. doi:10.1152/ajpendo.00165.2002.
74. **Krejza J**, **Mariak Z**, **Huba M**, **Wolczynski S**, **Lewko J.** Effect of endogenous estrogen on blood flow through carotid arteries. *Stroke* 32: 30–36, 2001. doi:10.1161/01.str.32.1.30.
75. **Krejza J**, **Siemkowicz J**, **Sawicka M**, **Szylak A**, **Kochanowicz J**, **Mariak Z**, **Lewko J**, **Spektor V**, **Babikian V**, **Bert R.** Oscillations of cerebrovascular resistance throughout the menstrual cycle in healthy women. *Ultrasound Obstet Gynecol* 22: 627–632, 2003. doi:10.1002/uog.907.
76. **Cote S**, **Butler R**, **Michaud V**, **Lavallee E**, **Croteau E**, **Mendrek A**, **Lepage JF**, **Whittingstall K.** The regional effect of serum hormone levels on cerebral blood flow in healthy nonpregnant women. *Hum Brain Mapp* 42: 5677–5688, 2021. doi:10.1002/hbm.25646.
77. **Howe CA**, **Caldwell HG**, **Carr J**, **Nowak-Fluck D**, **Ainslie PN**, **Hoiland RL.** Cerebrovascular reactivity to carbon dioxide is not influenced by variability in the ventilatory sensitivity to carbon dioxide. *Exp Physiol* 105: 904–915, 2020. doi:10.1113/EP088192.
78. **Hoiland RL**, **Fisher JA**, **Ainslie PN.** Regulation of the cerebral circulation by arterial carbon dioxide. *Compr Physiol* 9: 1101–1154, 2019. doi:10.1002/cphy.c180021.
79. **Raichle ME**, **Grubb RL Jr**, **Gado MH**, **Eichling JO**, **Ter-Pogossian MM.** Correlation between regional cerebral blood flow and oxidative metabolism. In vivo studies in man. *Arch Neurol* 33: 523–526, 1976. doi:10.1001/archneur.1976.00500080001001.
80. **Ibaraki M**, **Shinohara Y**, **Nakamura K**, **Miura S**, **Kinoshita F**, **Kinoshita T.** Interindividual variations of cerebral blood flow, oxygen delivery, and metabolism in relation to hemoglobin concentration measured by positron emission tomography in humans. *J Cereb Blood Flow Metab* 30: 1296–1305, 2010. doi:10.1038/jcbfm.2010.13.
81. **Ainslie PN**, **Shaw AD**, **Smith KJ**, **Willie CK**, **Ikeda K**, **Graham J**, **Macleod DB.** Stability of cerebral Metabolism and substrate availability in humans during hypoxia and hyperoxia. *Clin Sci (Lond)* 126: 661–670, 2014. doi:10.1042/CS20130343.
82. **Mathew RJ**, **Wilson WH.** Caffeine induced changes in cerebral circulation. *Stroke* 16: 814–817, 1985. doi:10.1161/01.str.16.5.814.
83. **Addicott MA**, **Yang LL**, **Peiffer AM**, **Burnett LR**, **Burdette JH**, **Chen MY**, **Hayasaka S**, **Kraft RA**, **Maldjian JA**, **Laurienti PJ.** The effect of daily caffeine use on cerebral blood flow: how much caffeine can we tolerate? *Hum Brain Mapp* 30: 3102–3114, 2009. doi:10.1002/hbm.20732.
84. **Frank S**, **Linder K**, **Kullmann S**, **Heni M**, **Ketterer C**, **Cavusoglu M**, **Krzeminski A**, **Fritsche A**, **Haring HU**, **Preissl H**, **Hinrichs J**, **Veit R.** Fat intake modulates cerebral blood flow in homeostatic and gustatory brain areas in humans. *Am J Clin Nutr* 95: 1342–1349, 2012. doi:10.3945/ajcn.111.031492.
85. **Tallroth G**, **Ryding E**, **Agardh CD.** Regional cerebral blood flow in normal man during insulin-induced hypoglycemia and in the recovery period following glucose infusion. *Metabolism* 41: 717–721, 1992. doi:10.1016/0026-0495(92)90310-7.
86. **Pires PW**, **Dams Ramos CM**, **Matin N**, **Dorrance AM.** The effects of hypertension on the cerebral circulation. *Am J Physiol Heart Circ Physiol* 304: H1598–H1614, 2013. doi:10.1152/ajpheart.00490.2012.
87. **Silvah JH**, **Marchini JS**, **Martires Lima CM**, **Ferreira Nicoletti C**, **Alexandre Santos L**, **Nobuyuki Itikawa E**, **Trevisan AC**, **Arriva Pitella F**, **Kato M**, **Iucif Junior N**, **Gai Frantz F**, **Freire Carvalho Cunha S**, **Buchpiguel CA**, **Wichert-Ana L.** Regional cerebral blood

flow at rest in obesity. *Nutrition* 79-80: 110888, 2020. doi:10.1016/j.nut.2020.110888.

88. **Rodriguez G**, **Bertolini S**, **Nobili F**, **Arrigo A**, **Masturzo P**, **Elicio N**, **Gambaro M**, **Rosadini G.** Regional cerebral blood flow in familial hypercholesterolemia. *Stroke* 25: 831–836, 1994. doi:10.1161/01.str.25.4.831.
89. **Carter KJ**, **Ward AT**, **Kellawan JM**, **Eldridge MW**, **Al-Subu A**, **Walker BJ**, **Lee JW**, **Wieben O**, **Schrage WG.** Nitric oxide synthase inhibition in healthy adults reduces regional and total cerebral macrovascular blood flow and microvascular perfusion. *J Physiol* 599: 4973–4989, 2021. doi:10.1113/JP281975.
90. **O'Gallagher K**, **Rosentreter RE**, **Elaine Soriano J**, **Roomi A**, **Saleem S**, **Lam T**, **Roy R**, **Gordon GR**, **Raj SR**, **Chowienczyk PJ**, **Shah AM**, **Phillips AA.** The effect of a neuronal nitric oxide synthase inhibitor on neurovascular regulation in humans. *Circ Res* 131: 952–961, 2022. doi:10.1161/CIRCRESAHA.122.321631.
91. **Peltonen GL**, **Harrell JW**, **Rousseau CL**, **Ernst BS**, **Marino ML**, **Crain MK**, **Schrage WG.** Cerebrovascular regulation in men and women: stimulus-specific role of cyclooxygenase. *Physiol Rep* 3, 2015. doi:10.14814/phy2.12451.
92. **Rundek T**, **Tolea M**, **Ariko T**, **Fagerli EA**, **Camargo CJ.** Vascular cognitive impairment (VCI). *Neurotherapeutics* 19: 68–88, 2022. doi:10.1007/s13311-021-01170-y.
93. **Cooper DB**, **Patel P**, **Mahdy H.** *Oral Contraceptive Pills*. Treasure Island, FL: StatPearls. 2023.
94. **O'Kelly AC**, **Michos ED**, **Shufelt CL**, **Vermunt JV**, **Minissian MB**, **Quesada O**, **Smith GN**, **Rich-Edwards JW**, **Garovic VD**, **El Khoudary SR**, **Honigberg MC.** Pregnancy and reproductive risk factors for cardiovascular disease in women. *Circ Res* 130: 652–672, 2022. doi:10.1161/CIRCRESAHA.121.319895.
95. **Conroy DA**, **Spielman AJ**, **Scott RQ.** Daily rhythm of cerebral blood flow velocity. *J Circadian Rhythms* 3: 3, 2005. doi:10.1186/1740-3391-3-3.
96. **Shariffi B**, **Lloyd IN**, **Cessac ME**, **Harper JL**, **Limberg JK.** Reproducibility and diurnal variation in middle cerebral artery blood velocity in healthy humans. *Exp Physiol* 108: 692–705, 2023. doi:10.1113/EP090873.